Journal of Power Sources 181 (2008) 120–126

Contents lists available at ScienceDirect

Journal of Power Sources

journal homepage: www.elsevier.com/locate/jpowsour

High performance rare earth oxides LnO_x (Ln = La, Ce, Nd, Sm and Dy)-modified Pt/SiO_2 catalysts for CO oxidation in the presence of H_2

Fang Wang[a,b], Gongxuan Lu[a,*]

[a] State Key Laboratory for Oxo Synthesis and Selective Oxidation, Lanzhou Institute of Chemical Physics, Chinese Academy of Sciences, Lanzhou 730000, PR China
[b] Graduate School of Chinese Academy of Sciences, Beijing 100039, PR China

ARTICLE INFO

Article history:
Received 22 January 2008
Received in revised form 18 March 2008
Accepted 18 March 2008
Available online 25 March 2008

Keywords:
CO oxidation
PROX
Pt/SiO_2
Rare earth oxide

ABSTRACT

The catalytic activities of low-temperature CO oxidation and preferential CO oxidation (PROX) in rich-H_2 stream over the Pt/SiO_2 and rare earth oxides modified Pt/SiO_2 catalysts have been investigated. The addition of rare earth oxide additives to the Pt/SiO_2 catalyst can promote the catalytic performance remarkably. The catalytic activities for PROX are dependent on the basicities of these oxides. The higher basic strength leads to higher activity. For $Pt–CeO_2/SiO_2$, the catalytic activity depends strongly on the content of CeO_2 and on the mole ratio of CO/O_2. XRD and H_2-temperature-programmed reduction (TPR) results show that the additives not only improve the dispersion of metallic Pt on the support surface, but also increase the reducibility of PtOx in $Pt–CeO_2/SiO_2$. The formation of the Pt–Ce alloy decreases the electron back-donation from the Pt 5d orbital to the $2\sigma^*$ orbital of CO, and consequently suppresses CO–Pt bonding, resulting in the lowered CO coverage.

1. Introduction

The CO oxidation in the absence and in the presence of H_2 has attracted extensive attention recently because of its potential application in indoor or cabin air cleanup and in the purification of hydrogen streams used in proton exchange membrane (PEM) fuel cells [1,2]. Hydrogen is usually produced by the catalytic steam reforming, partial oxidation, and auto-thermal reforming of hydrocarbons. However, CO is formed as a byproduct in all of these processes and must be subsequently removed prior to the introduction of hydrogen to PEM fuel cells, due to the fact that the high sensitivity of the Pt-based PEM electro-catalysts will be poisoned by CO [3–5]. The preferential oxidation of CO in the presence of hydrogen is recently considered as a potential method for hydrogen purification for PEM fuel cells.

Supported noble metals, such as Au [6–8], Pt [9–14], and Ru [15–17] were found applicable for the PROX reaction. Platinum catalysts are by far the most extensively studied catalysts [18–22]. In general, a suitable catalyst must adsorb CO and provide activated oxygen, while hydrogen adsorption must be suppressed. However, oxygen cannot adsorb on Pt surface when the surface is fully covered by CO (on Pt at $T < 440$ K [23,24]). Therefore, oxygen should be activated on different sites, either on the reducible support or on partially oxidized patches in the modified Pt catalysts. In this condition, oxygen will diffuse to interface sites and subsequently react either at the periphery, after a spillover process of one of the components, or on the adjacent metal/oxide site. Up to now, for the PROX reaction, it was known that addition of base metals (Na, K, and Cs) or transition metals (Co, Ni, and Cr) could significantly enhanced the activity of Pt catalysts, probably due to the changes in the adsorption characteristics of adsorbates either through electron transfer [25] or resulting bimetallic characteristics/effects [26].

Silica is considered as an excellent catalytic support in virtue of its desirable characteristics (inertness, high specific surface area, pronounced mesoporosity, and good thermal stability), which has been widely investigated for some reactions, such as CO methanation, hydrogenolysis of methylcyclopentane, and isomerization of 2-methylpentane [27,28].

In this work, SiO_2-supported Pt catalysts have been modified by adding rare earth oxides LnO_x (Ln = La, Ce, Nd, Sm, and Dy) to the Pt/SiO_2 catalysts that prepared using co-impregnation and sequential-impregnation methods. The obtained catalysts have been tested for CO oxidation both in H_2-free and H_2-rich environments. The effects of additives loadings were elucidated on the variation of basic strength of catalysts and the dispersion of metallic Pt on catalysts.

* Corresponding author. Tel.: +86 931 4968178; fax: +86 931 4968178.
E-mail address: gxlu@lzb.ac.cn (G. Lu).

0378-7753/$ – see front matter © 2008 Elsevier B.V. All rights reserved.
doi:10.1016/j.jpowsour.2008.03.040

2. Experimental

2.1. Catalyst preparation

Pt/SiO_2 was prepared by incipient wetness impregnation. Additives containing catalysts were prepared by co-impregnation or sequential-impregnation. In the process of sequential impregnation, SiO_2 (being calcined in air at 650 °C for 5 h) was first modified with Ln_2O_3 by the conventional wet impregnation method using $Ln(NO_3)_x$ (Ln = La, Ce, Nd, Sm and Dy) as the precursors, followed by drying overnight at 120 °C. The resulting Ln_2O_3/SiO_2 was then impregnated with $H_2PtCl_6{\cdot}6H_2O$ to prepare the $Pt/Ln_2O_3/SiO_2$. The resulting powder was dried overnight at 120 °C, followed by calcination at 500 °C for 4 h. The loading of Pt was 0.7% and the loadings of rare earth oxides were 5% in all catalysts.

2.2. Characterization of catalysts

Powder XRD analysis was performed to verify the species in the catalysts. XRD patterns of the samples were recorded on a Rigaku D/MAX-RB X-ray diffractometer with a Cu Kα target operated at 50 kV and 40 mA with a scanning speed of 0.5° min^{-1} and a scanning angle (2θ) range of 10–90°. H_2-TPR of the catalyst was performed at atmospheric pressure in a conventional flow system built in our laboratory at a linearly programmed rate of 10 °C min^{-1} from 20 °C to 800 °C (5% H_2 in a Ar stream with a flow rate of 40 mL min^{-1}). Sample of 50 mg was used for each run. The amount of the consumed H_2 was determined by a thermo-conductivity detector (TCD). Before each measurement, the samples were purged with dry air at 400 °C for 1 h.

2.3. Activity–selectivity measurement

Catalytic performances tests were carried out in a fixed bed continuous flow quartz reactor (i.d. 5 mm) under a normal pressure from 60 °C to 200 °C. Typically, 100 mg of the catalyst was used in each run. All the catalysts were reduced in situ by 50% H_2 in a N_2 stream at 500 °C for 1 h prior to use. The total flow rate of the feed gas was 60 ml min^{-1} (GHSV = 36,000 h^{-1}). The feed gas consisted of 1.5% of CO and 20% O_2 in N_2 balance. In the process of PROX, a gas mixture containing 50% H_2, 1% CO and 2% O_2 in N_2 was feed at the flow rate of 30 ml min^{-1}. Argon was used as the carrier gas and nitrogen was used as the internal standard for gas analysis. The gas phase effluents were analyzed on-line chromatographs equipped with TCD. At the end of the catalytic tests, the catalyst was cooled under an N_2 stream and stored for characterizations. The catalytic activities were defined in terms of conversion of CO, conversion of O_2 and selectivity to CO_2. Which were denoted as CO%, O_2%, and S%, respectively, and were calculated according to the corresponding equations:

$$\mathrm{CO}(\%) = \frac{[\mathrm{CO}]_{in}-[\mathrm{CO}]_{out}}{[\mathrm{CO}]_{in}} \times 100$$

$$\mathrm{O_2}(\%) = \frac{[\mathrm{O_2}]_{in}-[\mathrm{O_2}]_{out}}{[\mathrm{O_2}]_{in}} \times 100$$

$$\mathrm{S}(\%) = \frac{0.5\times[\mathrm{CO_2}]}{[\mathrm{O_2}]_{in}-[\mathrm{O_2}]_{out}} \times 100$$

3. Results and discussion

3.1. Characterization of catalysts

3.1.1. XRD

Fig. 1 shows the XRD patterns of original Pt/SiO_2 and rare earth oxide modified ones. It is clear that all the samples contain the framework of SiO_2. The characteristic diffraction peaks of Pt appear at 39.68°, 46.18°, 67.36°, and 81.21° (2θ) in the Pt/SiO_2 catalyst (a),

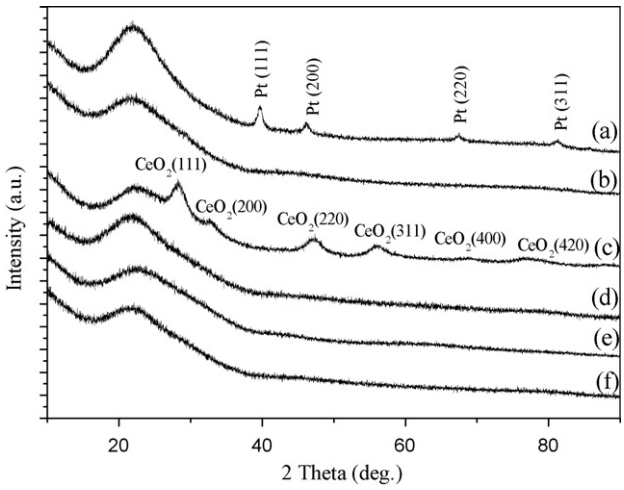

Fig. 1. XRD patterns of the original Pt/SiO_2 catalyst and various rare earth oxides modified ones. (a) Pt/SiO_2, (b) $Pt–La_2O_3/SiO_2$, (c) $Pt–CeO_2/SiO_2$, (d) $Pt–Nd_2O_3/SiO_2$, (e) $Pt–Sm_2O_3/SiO_2$, and (f) $Pt–Dy_2O_3/SiO_2$.

which correspond to the (1 1 1), (2 0 0), (2 2 0), and (3 1 1) faces. However, characteristic diffraction peak of Pt is not found in the catalysts containing rare earth oxides. According to the polycrystalline XRD theory, the weaker the diffraction peak, and the smaller the dimension of Pt particles is. That is to say, the addition of various rare earth oxides improves the dispersion of Pt species over SiO_2, which may be one of the reasons for the high activity of the modified Pt/SiO_2 catalysts.

In addition, we can see that except the CeO_2-modified Pt/SiO_2 catalyst, characteristic diffraction peaks of the rare earth oxides are not found in the modified catalysts. This result indicates that rare earth oxides partly transferred from surface into SiO_2, and further reduce to the amount which is below detection limit. The removal decreases the interface between the rare earth oxide and Pt, however, the interface is essential for the oxygen activity and the adsorption of CO. Therefore, this may be one of the reasons why the activity of CO oxidation on the CeO_2-modifed Pt/SiO_2 is much higher than that of the other rare earth oxides modified ones.

3.1.2. H_2-TPR

The catalyst can be reduced and oxidized in our fixed bed system for CO oxidation and PROX.

Thus, the catalyst reducibility is evaluated by measuring the temperature-programmed reduction. H_2-TPR profiles of the original Pt/SiO_2 catalyst and rare earth oxides modified ones are shown in Fig. 2. The Pt/SiO_2 catalyst (a) shows a reduction peak at 400 °C and a poorly resolved reduction peak expanded from 500 °C to 750 °C. This result suggests that the formation of isolated metallic Pt species requires a higher temperature. The consumption of hydrogen indicates that an almost complete reduction to metallic platinum occurs, which means that most of the platinum species interact strongly with the support. The reduction peaks of Pt move towards lower temperatures to certain extent with the addition of rare earth oxides. The reduction peaks of Pt, on the La_2O_3 (b), CeO_2 (f), Nd_2O_3 (c), Sm_2O_3 (d), and Dy_2O_3 (e) modified catalysts appear at about 300 °C, 350 °C, 280 °C, 275 °C and 190 °C, respectively. Moreover, the reduction peaks of Pt are all asymmetric peaks which indicating there are more than one PtOx species on the catalyst. Compared with the other modified catalysts, a double reduction peak on the catalyst $Pt–CeO_2/SiO_2$ is observed. The result indicates that not only Pt is reduced, but CeO_2 is also partly reduced.

Furthermore, effect of the content of CeO_2 on the reducibility of $Pt–CeO_2/SiO_2$ catalysts is also investigated. Fig. 3 shows the H_2-TPR

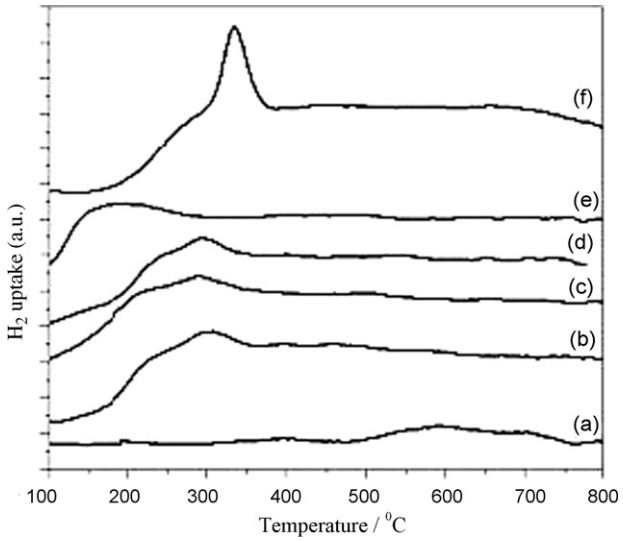

Fig. 2. H_2-TPR profiles for (a) Pt/SiO_2, (b) $Pt–La_2O_3/SiO_2$, (c) $Pt–Nd_2O_3/SiO_2$, (d) $Pt–Sm_2O_3/SiO_2$, (e) $Pt–Dy_2O_3/SiO_2$, and (f) $Pt–CeO_2/SiO_2$.

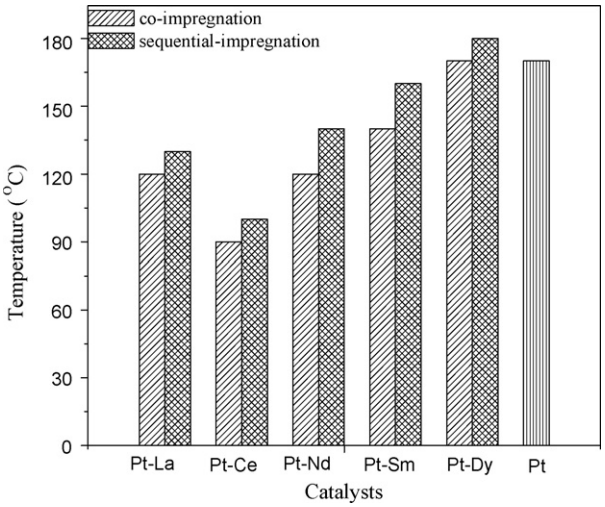

Fig. 4. The minimum temperatures for CO convert completely in the absence of H_2 over the original Pt/SiO_2 catalyst and various rare earth oxides modified ones prepared by different impregnation methods.

patterns of the series of $Pt–CeO_2/SiO_2$ catalysts containing different amounts of CeO_2. In order to compare with $Pt–CeO_2/SiO_2$ catalysts, the H_2-TPR profile of CeO_2/SiO_2 (b) is also shown in Fig. 3. In the CeO_2-modified Pt/SiO_2 samples with lower CeO_2 contents (c–e) (1–5%), the reduction temperatures of Pt species are greatly reduced. For example, on $Pt1CeO_2/SiO_2$ catalyst (c), the TPR profile shows a reduction peaks at 200 °C, which indicates the reduction of Pt species in the catalysts takes place largely under mild conditions. Moreover, a subsequent TPR analysis of the samples has not shown any further hydrogen consumption. Therefore, it is possible to infer that only metallic Pt species are present on the surface at the activation temperature of our systems (500 °C).

It is interesting to note that a broad H_2-consumption peak is detected when the CeO_2 content reaches 7–10%. For the reduction profile of $Pt–7CeO_2/SiO_2$ (f), in addition to the low-temperature reduction peaks related to Pt–Ce species, a broad peak centred at about 450 °C and 550 °C is also detected. The low-temperature components probably correspond to an initial formation of metallic Pt or Pt-rich alloys; the high-temperature reduction partially involves the unalloyed ceria that catalyzed by the presence of noble metal. It is necessary to have the detailed quantum-mechanical information about the bonding mechanism between Pt and the bulk alloy. The relative low electronic density of the d-band in the Pt skin can be easily understood in terms of the orbital mixing. Hybridization of the occupied states of an electron-rich metal (Pt) with the unoccupied levels of an electron-poor metal (Ce or bulk alloy) leads to the loss of the Pt character in the occupied states and hence to the reduction in the electron density on the Pt skin. On the basis of the results, we propose a mechanism for the CO tolerance, i.e., the lowered electron density of the 5d orbital of Pt decreases an electron back-donation from the Pt 5d orbital to the $2\sigma^*$ orbital of CO, and consequently suppresses the CO–Pt bonding, results in the lowered CO coverage.

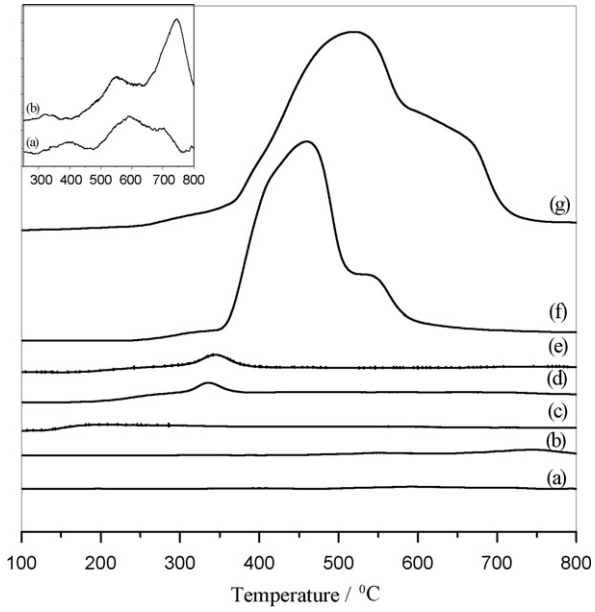

Fig. 3. H_2-TPR profiles for (a) Pt/SiO_2, (b) CeO_2/SiO_2, (c) $Pt–1CeO_2/SiO_2$, (d) $Pt–3CeO_2/SiO_2$, (e) $Pt–5CeO_2/SiO_2$, (f) $Pt–7CeO_2/SiO_2$, and (g) $Pt–10CeO_2/SiO_2$.

Furthermore, the intensity of this H_2-consumption peak gradually enhances with the increase of CeO_2 amount (see Fig. 3). It is due to the reduction of the special oxygen species. The reduction peaks of lattice oxygen of CeO_2 supported on SiO_2 appear at 320 °C, 540 °C and 750 °C (b). Therefore, the special oxygen species in the active centres exhibit different properties in comparison with the lattice oxygen of pure CeO_2. Compared with the lattice oxygen of pure CeO_2, the special oxygen species is more active and more easily reduced by hydrogen. The special oxygen species play an important role in the oxidation of CO.

3.2. Activity test

3.2.1. Influence of auxiliary agents and preparation methods

The comparisons of the minimum temperatures for CO elimination on the different catalysts that prepared by co-impregnation and sequential impregnation methods are shown in Fig. 4. The results show that activities are very sensitive to preparation procedures. Performances of co-impregnated catalysts are superior to those of the sequential impregnated ones. The additive effect of dysprosium oxide is very poor, the catalytic activity for CO oxidation is slightly lower than that of the Pt/SiO_2 one, especially in the $Pt–Dy_2O_3/SiO_2$ catalyst prepared by the sequential impregnation method. However, the effects of other rare earth oxides are great. Fig. 5 shows the CO oxidation activity of the

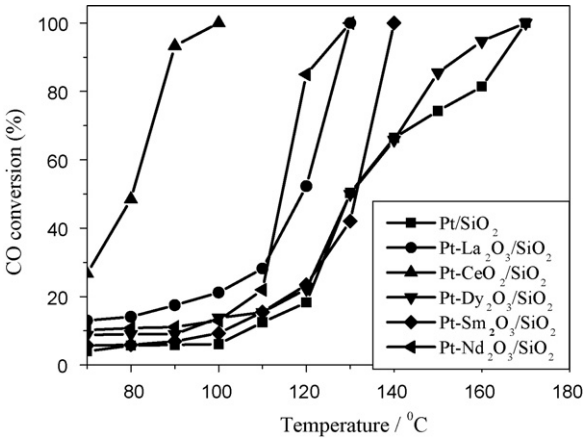

Fig. 5. Relation between reaction temperature and conversion for CO oxidation in the absence of H_2 over the original Pt/SiO_2 catalyst and various rare earth oxides modified ones prepared by co-impregnation method (CO concentrations in the effluent gas are 1.5 vol.% CO, 20 vol.% O_2, and N_2 balance).

original Pt/SiO_2 catalyst and the modified ones that prepared by the co-impregnation method. Activities of the co-impregnated catalysts for CO oxidation in the absence of H_2 decrease in the order of $Pt–CeO_2 > Pt–La_2O_3 \sim Pt–Nd_2O_3 > Pt–Sm_2O_3 > Pt–Dy_2O_3 \sim Pt$. The oxygen mobility on the oxide support appears to have a major impact on the catalyst performance in the CO oxidation reaction. Other authors [29,30] have shown that surface oxygen atoms from ceria do participate in the oxidation of CO at low temperature.

The performance of the catalysts for PROX in the presence of H_2 was also tested. The experiments were carried out with a GHSV of 12,000 h^{-1}, and a gas composition of 1 vol.% of CO, 50 vol.% of H_2, 2 vol.% of O_2 and N_2 (to balance). Fig. 6(I) shows the CO conversion versus temperature curves for various catalysts. On the Pt/SiO_2 catalyst, CO does not convert completely until the reaction temperature increase to 200 °C. It is clearly indicated that the original Pt/SiO_2 catalyst shows a low activity. Upon the addition of the rare earth oxide to Pt/SiO_2, the conversion of CO is greatly increased compared with the original Pt/SiO_2 one. The extent of increment depends on the choice of the rare earth oxide used. The minimum temperatures for CO complete oxidation (T_{100}) on La_2O_3, Nd_2O_3, Sm_2O_3 and Dy_2O_3-modified Pt/SiO_2 catalysts are 140 °C, 150 °C, 160 °C and 180 °C, respectively. The CeO_2-modified Pt/SiO_2 catalyst has the highest activity, and CO can convert completely at a low temperature of 110 °C. Maitra [31] had reported relative basicities of the rare earth oxides (Ln_2O_3) decrease in the following order: La > Pr ~ Nd > Sm > Gd ~ Eu > Tb ~ Ho ~ Er > Dy ~ Tm ~ Yb ~ Lu > Ce. Thus, except the CeO_2-modified Pt/SiO_2 catalyst, this classification does perfectly match the basicity scale for these oxides, and effect of the additives is similar with that in the CO oxidation process. This is consistent with the result that the samples prepared on basic supports are more active for the CO oxidation reaction than the corresponding samples supported on acidic ones [32,33]. Furthermore, a correlation between the oxygen surface diffusion coefficient and basicity of these oxides has also been reported [34]. On the other hand, the common method for the preparation of Pt/SiO_2 catalysts involves electrostatic adsorption, where the point of zero charge (PZC) of silica determines the adsorption ability of Pt precursors according to the charge attraction [35]. In general, a lower isoelectric point of SiO_2 (IEP~2) implying that the surface is highly negatively charged and chloroplatinic acid (H_2PtCl_6) does not strongly adsorbed on silica. Thus, suitable additives should be investigated in order to bring about the occurrence of a higher IEP under proper deposition conditions. The IEPs of the rare earth oxides, such as La_2O_3 and CeO_2, are much higher

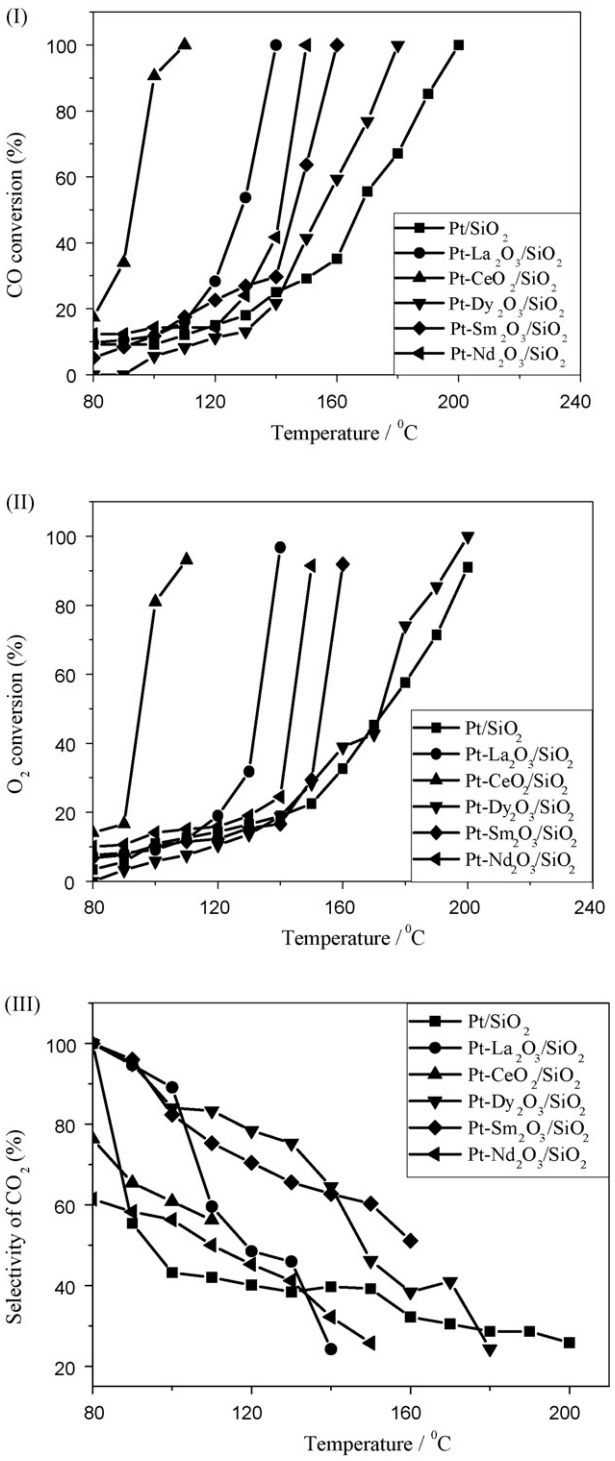

Fig. 6. Reaction temperature dependence of CO conversion (I), O_2 conversion (II), and selectivity of CO_2 (III) of PROX in H_2-rich gas over different catalysts. (CO concentrations in the effluent gas are 1.0 vol.% CO, 2 vol.% O_2 and 50 vol.% H_2 (N_2 balance)).

than that of SiO_2; therefore, the addition of rare earth oxides may increase the IEP of SiO_2 to a certain extent. The change is beneficial to the adsorption of metal platinum on SiO_2 and further to the promotion of the CO oxidation activity. Fig. 6(II) shows that the tendency of O_2 conversion on all the catalysts tested is similar to that of CO conversion. The selectivity of CO_2, however, as shown in Fig. 6(III), decreases with the increasing reaction temperature.

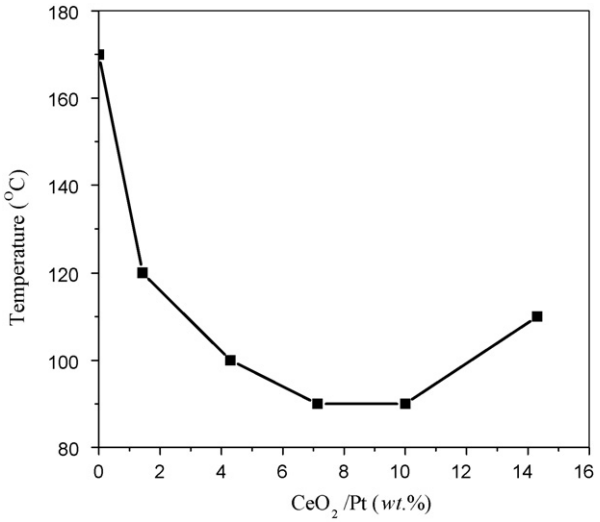

Fig. 7. Relation between the content of CeO_2 and the minimum temperatures for CO elimination over the Pt–CeO_2/SiO_2 catalysts for CO oxidation in the absence of H_2 (CO concentrations in the effluent gas are 1.5 vol.% CO, 20 vol.% O_2 and N_2 balance).

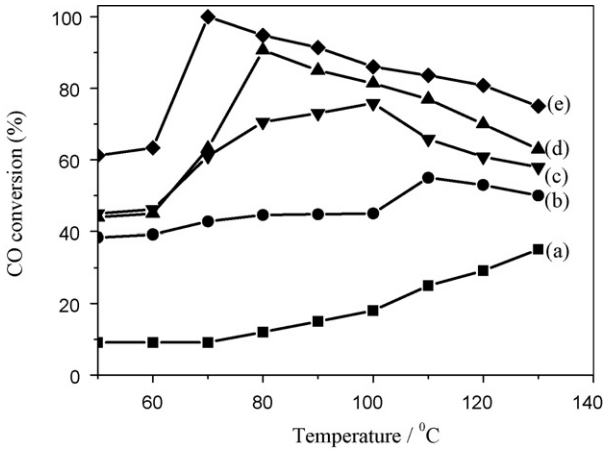

Fig. 8. Reaction temperature dependence of CO conversion of PROX in H_2-rich gas over the Pt–CeO_2/SiO_2 catalysts containing different amount of CeO_2. (a) Pt/SiO_2, (b) Pt–1CeO_2/SiO_2, (c) Pt–3CeO_2/SiO_2, (d) Pt–7CeO_2/SiO_2, and (e) Pt–10CeO_2/SiO_2 (CO concentrations in the effluent gas are 1.0 vol.% CO, 2 vol.% O_2, and 50 vol.% H_2 (N_2 balance)).

On account of the highest catalytic activity in all the catalysts investigated, the ceria modified Pt/SiO_2 catalyst was also studied in this paper.

3.2.2. *Effect of CeO_2 content on catalytic performance of Pt–CeO_2/SiO_2 for CO oxidation in the absence of H_2*

In order to elucidate the excellent properties of the co-impregnated catalysts and reveal the relationship between material structure and catalytic performance, co-impregnated Pt–CeO_2/SiO_2 catalysts with different Pt–CeO_2 compositions were prepared, and reaction conditions for CO oxidation have been investigated in detail. Fig. 7 illustrates the influence of CeO_2/Pt weight ratio on the CO oxidation activity of the CeO_2-modified Pt/SiO_2 catalyst. The amount of Pt loaded is kept at 0.7 wt%, while that of CeO_2 changes. It is clearly shown that Pt/SiO_2 catalyst shows a low activity and the minimum temperature of CO complete oxidation is 200 °C. The Pt–CeO_2/SiO_2 catalysts exhibit relatively high activity than that of the Pt single supported one. The minimum temperature of CO elimination is drastically decreased by the addition of a small amount of CeO_2 with a CeO_2/Pt ratio of 1.43. With the further increase of CeO_2/Pt ratio, the temperature decreases gradually and then keeps stable at around a CeO_2/Pt ratio of 7.14–10. But the addition of CeO_2 in excess does not always decrease the minimum temperature of CO elimination. When the CeO_2/Pt ratio increases to 14.3, the temperature of CO converts completely increases to 110 °C, accordingly. It seems that the partly coverage of Pt in the Pt–10CeO_2/SiO_2 catalyst during preparation is accounted for their lower activity.

3.2.3. *Influence of CeO_2 content on catalytic performance of Pt–CeO_2/SiO_2 for PROX in rich-H_2 streams*

CO conversion versus temperature curves obtained in these experiments for the Pt/SiO_2 catalysts modified by different amounts of ceria (Fig. 8) is given as a representative of these experiments. (O_2 conversion and selectivity of CO_2 vs. temperature curves are not given in this paper). All the curves in Fig. 8 present an initial increase of CO conversion with temperature, and after reaching a maximum a progressive decay can be observed as the temperature rises. The increase in activity is found to be very obvious at low temperature but it approaches zero at high temperature [36,37]. This supports the mechanism in which the promoter activates the oxygen required for the reaction: at low temperatures, oxygen is activated at the interface when Pt is completely covered by CO, whereas at higher temperatures oxygen can also be activated on Pt sites. Comparing the PROX behavior of these catalysts, we can see that the one with the highest content of CeO_2 is the most active catalyst investigated, and catalytic activities decrease in the following order: Pt10CeO_2 > Pt7CeO_2 > Pt3CeO_2 > Pt1CeO_2 > Pt. Thus, all the catalysts modified by CeO_2 exhibit higher activities than the origin Pt/SiO_2 one because the former contributes Pt–CeO_2 interface to the activity (this is consistent with the XRD result), which acts as atomic oxygen supplier.

Maximum CO conversion temperature (T_{max}), CO conversion and the selectivity of CO_2 at that temperature are given for comparison in Table 1. According to the selectivity increases with the increase of CeO_2 content in the modified catalysts, we propose that the preferential oxidation of CO over CeO_2-modified Pt/SiO_2 catalysts can occur via a non-competitive Langmuir–Hinshelwood mechanism. Such a mechanism involves the reaction between the CO adsorbed on the Pt metal particles and the oxygen atoms previously activated on the support. The activated oxygen on the original Pt/SiO_2 catalyst originates from the adsorbed oxygen, however, on Pt–CeO_2/SiO_2, the surface oxygen atoms from ceria are also participating in the PROX reaction process. In addition, the selectivity of CO_2 decreases as the reaction temperature increases, in virtue of the fact that CO completely covers the metallic Pt surface and CO oxidation takes place mainly at low temperature. However, when the temperature rises, CO desorption from Pt surface becomes important and it is partially replaced by H_2, this effect favors H_2 oxidation.

Comparing the behavior of the catalysts in the absence and presence of H_2 (Figs. 7 and 8 and Table 1), it is interesting to note that

Table 1
Values of the temperature for maximum CO conversion (T_{max}), maximum CO conversion, O_2 conversion and selectivity of CO_2 at T_{max} in H_2-rich conditions for the catalysts containing different amount of CeO_2

Catalysts	Metal loading (wt%)		Feed stream with 50% H_2		
	Pt	CeO_2	T_{max} (°C)	X_{CO} (%)	Selectivity (%)
Pt/SiO_2	0.7	0	200	100	25.8
Pt–1CeO_2/SiO_2	0.7	1	110	55	48.3
Pt–3CeO_2/SiO_2	0.7	3	100	75.8	52.3
Pt–5CeO_2/SiO_2	0.7	5	90	90.6	56.2
Pt–7CeO_2/SiO_2	0.7	7	90	100	70.8
Pt–10CeO_2/SiO_2	0.7	10	70	100	71.2

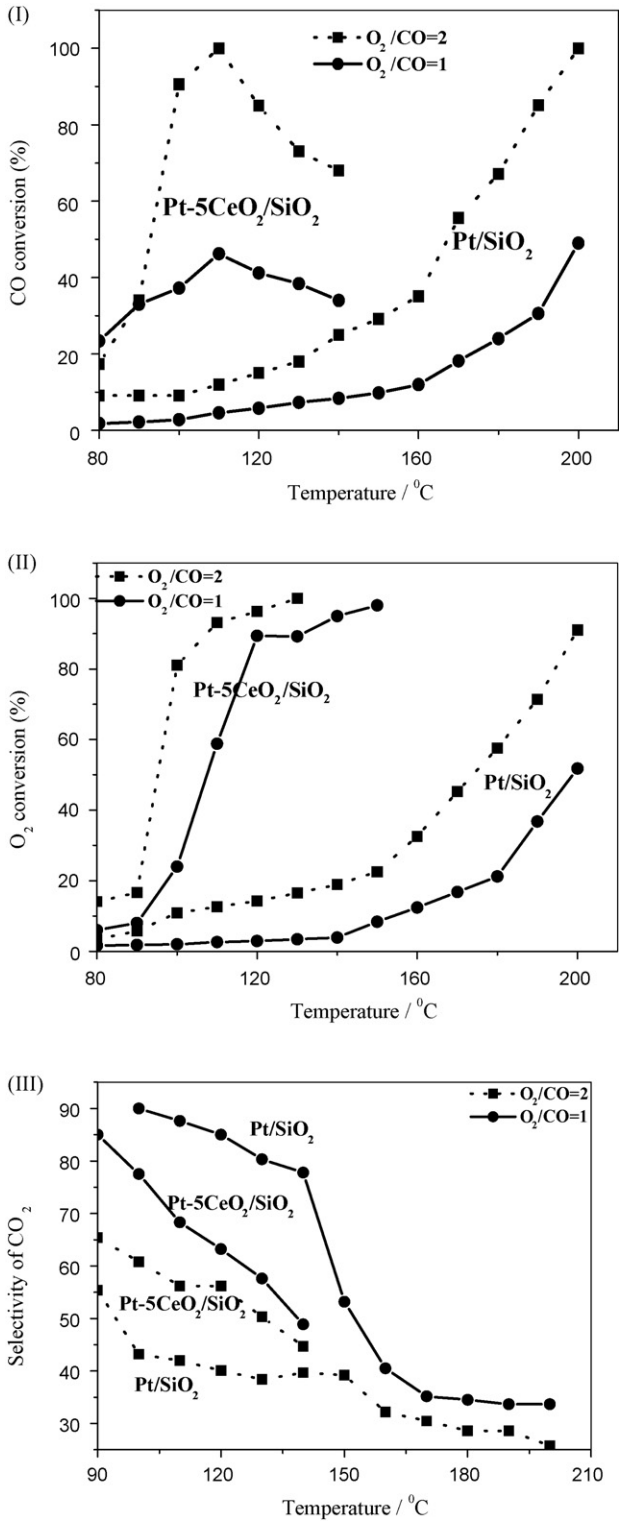

Fig. 9. CO conversion (I), O_2 conversion (II) and selectivity of CO_2 (III) over Pt/SiO_2 and $Pt–5CeO_2/SiO_2$ dependence of the different mole ratios of O_2/CO.

the catalytic activity for PROX in the presence of H_2 does increase linearly with increase in the content of CeO_2 from 1% to 10%, which is different from that for CO oxidation in the absence of H_2. This is maybe the addition of CeO_2 strongly enhances the activity of the water gas shift reaction (WGSR) in the process of PROX in the presence of H_2, and therefore CO conversion is also increased. Moreover, we can see that the maximum CO conversion temperatures for all catalysts shift to higher temperatures in the presence of H_2. Thus, Hydrogen cannot enhance CO oxidation just as reported in the previously article [32]. The relative positions of the curves can be related to the total amount of Pt (Langmuir–Hinshelwood mechanism) and $Pt–CeO_2$ interface (dual-site mechanism, involving the atomic oxygen supply to the reaction) when the experimental conditions are more oxygen-demanding than those in the absence of H_2. Sirijaruphan et al. [36] having studied a Fe-promoted Pt/Al_2O_3 catalyst, also suggested that a promoter does not increase the number of active sites, and the activity is controlled by the Pt-oxide interface.

3.2.4. *Effect of mole ratio O_2/CO*

The influence of the gas composition is also checked. CO conversion, O_2 conversion and the selectivity of CO_2 for Pt/SiO_2 and $Pt–5CeO_2/SiO_2$, as functions of λ (varied from 1 to 2) are shown in Fig. 9. We can see that the maximum value of CO conversion obtained strongly depends on λ, the higher the λ value, the higher the maximum CO conversion. When a stoichiometric amount of oxygen is added (λ = 1), a maximum CO conversion of 46.2% over $Pt–5CeO_2/SiO_2$ is achieved, which indicate that the λ value of 1 is not enough to achieve the total CO conversion with this catalyst in the presence of H_2. Therefore, the total CO conversion is obtained at 110 °C when a λ value of 2 is used. However, CO conversion on Pt/SiO_2 increases monotonously with the reaction temperature. O_2 conversions for λ = 1 and 2 are shown in Fig. 9(II), the tendency is different from that of CO conversion and the selectivity of CO_2. The O_2 conversions on both the catalysts increase with the increasing temperature in the range of reaction temperature investigated. These results indicate that both CO and H_2 oxidations increase as λ increases, however, the effect of the excess of oxygen is much more pronounced on the hydrogen oxidation. As a result, the selectivity of CO_2 decreases as the excess of oxygen increases. As shown in Fig. 9(III), the selectivity of CO_2 over $Pt–5CeO_2/SiO_2$, corresponding to the maximum CO conversion temperature is inversely proportional to λ value, with 56.2% for λ = 2, and 68.3% for λ = 1.

Comparing the results in Fig. 9 and Table 1, we can deduce that increasing the amount of CeO_2 added to a Pt/SiO_2 catalyst can increase the selectivity of CO_2, which is just the same effect as decrease of the λ value. Thus, the addition of CeO_2 to the base catalyst Pt/SiO_2 will allow using a smaller amount of oxygen in actual application. It is not clear whether a higher amount of CeO_2 can improve the performance for λ = 2 or not. This effect should be studied and optimized, which is mainly related to the amount of the formed $Pt–CeO_2$ interface.

4. Conclusions

The catalytic activities of the original and rare earth oxide modified Pt/SiO_2 catalysts for CO oxidation and PROX in rich-H_2 streams were investigated. The catalytic activities for CO oxidation in the presence of H_2 decrease in the following order: $Pt–CeO_2 > Pt–La_2O_3 > Pt–Nd_2O_3 > Pt–Sm_2O_3 > Pt–Dy_2O_3 > Pt$. The results indicate that, on the one hand, catalytic activity depends dramatically on the basicity of rare earth oxides, this is maybe due to the correlation between the oxygen surface diffusion coefficient and basicity of oxides, and the activated oxygen is essential in the process of CO oxidation. On the other hand, additives increase the IEP of the surface of silica. XRD result shows that the addition of rare earth oxides improves the dispersion of Pt species on the surface of silica. In addition, on account of the highest activity in all the catalysts investigated, $Pt–CeO_2/SiO_2$ was also studied in detail. It is interesting to note that the catalytic activity for

PROX in presence of H_2 does increase linearly with the content of CeO_2 increased from 1% to 10%, which is different from that for CO oxidation in the absence of H_2. Maybe, the addition of CeO_2 enhances the activity of WGSR in certain extent and, therefore, the conversion of CO in the process of PROX also increases. TPR results show that the reduction peak of Pt species shifts towards lower temperature with the addition of rare earth oxides, simultaneously, the reduction peak of Pt–Ce alloy is also found in the TPR profiles of $Pt–CeO_2/SiO_2$ catalyst. Therefore, we can infer that the formation of Pt–Ce alloy maybe responsible for the better catalytic performance of $Pt/SiO_2–CeO_2$.

Acknowledgment

The 973 (G20000264) Research Fund is acknowledged for financial support for this work.

References

[1] A.K. Santra, D.W. Goodman, Electrochim. Acta 47 (2002) 3595–3609.
[2] Z.C. Tang, D.S. Geng, G.X. Lu, J. Colloid Interface Sci. 287 (2005) 159–166.
[3] W.A. Adams, J. Blair, K.R. Bullock, C.L. Gardner, J. Power Sources 145 (2005) 55–61.
[4] R.J. Farrauto, M. Flytzani-Stephanopulos, Adsorbents and Electrocatalysts, Elsevier, Amsterdam, 2005.
[5] D.S. Geng, G.X. Lu, J. Phys. Chem. C 111 (2007) 11897–11902.
[6] G. Avgouropoulos, T. Ioannides, Ch. Papadopoulou, J. Batista, S. Hocevar, H.K. Martalis, Catal. Today 75 (2002) 157–167.
[7] D.S. Geng, G.X. Lu, J. Nanoparticle Res. 9 (2007) 1145–1151.
[8] M.J. Kahlich, H. Gasteiger, R.J. Behm, J. Catal. 182 (1999) 430–440.
[9] M.M. Schubert, M.J. Kahlich, H.A. Gasteiger, R.J. Behm, J. Power Sources 84 (1999) 175–182.
[10] S.H. Oh, R.M. Sinkevitch, J. Catal. 142 (1993) 254–262.
[11] M.J. Kahlich, H.A. Gasteiger, R.J. Behm, J. Catal. 171 (1997) 93–105.
[12] S. Özkara, A.E. Aksoylu, Appl. Catal. A: Gen. 251 (2003) 75–83.
[13] D.S. Geng, L. Chen, G.X. Lu, J. Mol. Catal. A 265 (2007) 42–49.
[14] Z.C. Tang, D.S. Geng, G.X. Lu, Thin Solid Films 497 (2006) 309–314.
[15] Y.F. Han, M. Kinne, R.J. Behm, Appl. Catal. B: Environ. 52 (2004) 123–134.
[16] M. Echigo, T. Tabata, Appl. Catal. A: Gen. 251 (2003) 157–166.
[17] Y.F. Han, M.J. Kahlich, M. Kinne, R.J. Behm, Phys. Chem. Chem. Phys. 4 (2002) 389–397.
[18] O. Korotkikh, R. Farrauto, Catal. Today 62 (2000) 249–254.
[19] H. Igarashi, H. Uchida, M. Suzuki, Y. Sasaki, M. Watanabe, Appl. Catal. A: Gen. 159 (1997) 159–169.
[20] M. Kotobuki, A. Watanabe, H. Uchida, H. Yamashita, M. Watanabe, J. Catal. 236 (2005) 262–269.
[21] I. Rosso, C. Galletti, G. Saracco, E. Garrone, V. Specchia, Appl. Catal. B: Environ. 48 (2004) 195–203.
[22] H. Kim, M. Lim, Appl. Catal. A: Gen. 224 (2002) 27–38.
[23] M.M. Schubert, M.J. Kahlich, G. Feldmeyer, M. Hüttner, S. Hackensberg, H.A. Gasteiger, R.J. Behm, Phys. Chem. Chem. Phys. 3 (2001) 1123–1131.
[24] X. Liu, O. Korotkikh, R. Farrauto, Appl. Catal. A: Gen. 226 (2002) 293–303.
[25] J. Günster, R. Souda, Chem. Phys. Lett. 371 (2003) 534–539.
[26] C. Kwak, T.J. Park, D.J. Suh, Appl. Catal. A: Gen. 278 (2005) 181–186.
[27] H. Miura, R.D. Gonzalez, J. Catal. 74 (1982) 216–224.
[28] G. Diaz, F. Garin, G. Maire, S. Alerasool, R.D. Gonzalez, Appl. Catal. A 124 (1995) 33–46.
[29] T. Bunluesin, G. Graham, R. Gorte, Appl. Catal. B: Environ. 14 (1997) 105–115.
[30] R. Taha, D. Martin, S. Kacimi, D. Duprez, Catal. Today 29 (1996) 89–92.
[31] A.M. Maitra, J. Therm. Anal. Calorim. 36 (1990) 657–675.
[32] J.L. Ayastuy, M.P. González-Marcos, J.R. González-Velasco, M.A. Gutiérrez-Ortiz, Appl. Catal. B: Environ. 70 (2007) 532–541.
[33] F. Mariño, C. Desrome, D. Duprez, Appl. Catal. B: Environ. 54 (2004) 59–66.
[34] D. Martin, Ph.D. Thesis, Poitiers University, 1994.
[35] M. Schreier, J.R. Regalbuto, J. Catal. 225 (2004) 190–202.
[36] A. Sirijaruphan, J.G. Goodwin, R.W. Rice, J. Catal. 224 (2004) 304–313.
[37] K. Tanaka, Y. Morooka, K. Ishigure, T. Yajuma, Y. Okabe, Y. Kato, H. Hamano, S. Sekiya, H. Tanaka, Y. Matsumoto, H. Koinuma, H. He, C. Zhang, Q. Feng, Catal. Lett. 92 (2004) 115–121.